Electron and positron scattering from the benzene derivative benzotrifluoride: Total and vibrational excitation cross sections

H. Kato,[1] S. Kobayashi,[1] C. Makochekanwa,[1,2,*] M. Hoshino,[1] N. Shinohara,[3] O. Sueoka,[2] H. Cho,[4] and H. Tanaka[1]
[1]*Department of Physics, Sophia University, Tokyo 102-8554, Japan*
[2]*Faculty of Engineering, Yamaguchi University, Yamaguchi 755-8611, Japan*
[3]*School of Medicine, Yamaguchi University, Yamaguchi 755-8505, Japan*
[4]*Department of Physics, Chungnam National University, Daejeon 305-764, South Korea*
(Received 20 December 2008; published 4 June 2009)

Electron and positron cross sections have been investigated experimentally for scattering from benzotrifluoride ($C_6H_5CF_3$) molecules over the energy range 0.2–1000 eV. The current results have been compared with our previous results for C_6H_6 molecules. Similar to C_6H_6, a peak has been observed in electron total cross sections (TCS) centered at 8.0 and a shoulder at about 40 eV. Vibrational excitation cross section experiments were carried out to probe the origin and nature of the 8 eV peak. For positron TCS, a broad peak spanning the region 0.8–15 eV and a change in slope at about 40 eV are observed with the only difference between the current results and those of C_6H_6 observed in the region 1–100 eV.

DOI: 10.1103/PhysRevA.79.062702 PACS number(s): 34.80.Bm, 34.80.Dp, 36.10.Dr

I. INTRODUCTION

We have interests in gaining insights into the substitutional effects on benzene (C_6H_6) as models of unsaturated systems, so that a general principle may be extracted for better understanding of the electronic as well as geometrical molecular-structure effects on electron and positron scattering. The earliest theoretical works on benzene consistently observed in excitation cross sections that π electrons are clearly easy to promote to the lowest excited levels [1,2]. The substitution of any H atom(s) from the benzene molecular-structure results in either donation or extraction of electron(s) to or from the benzene ring with significant effects on the physical and chemical properties of the resulting molecules, for example, electron affinities [3], thermal electron mobilities [4], rate constants for electron attachment [5], and basicities [6]. Some interesting phenomena that have been observed so far to be characteristic of these benzene-derived molecules include (i) the lifting of the degeneracy of the two lowest unoccupied π orbitals, compared to benzene, (ii) shifts in the positions of the peaks corresponding to compound-negative-ion states observed in threshold-electron-excitation spectra [7], and (iii) enhancement of scattering cross sections due to the additional contribution from electron attachment (see [8,9] and references therein). In general, electron capture by these molecules involves π^* molecular orbitals and thus serves as a probe of the effect of the substitution of an H atom by an atom or radical upon the orbital energies.

Our group has so far carried out systematic studies of the benzene H atom(s) substitutional effects to the electron and positron scattering properties of the resulting molecules. These started by the investigation of electron and positron total cross sections (TCS) [10] and electron impact elastic differential cross sections (DCS) [11] of the "parent molecule" C_6H_6 over the energy range of 0.2–1000 eV. Electron and positron scattering TCS were studied for the effects due to a single H atom replacement from the benzene ring by an F atom [12] and a Cl atom [13]. In the work of Ref. [12] we also investigated the effects of (i) replacing two H atoms from the benzene ring by two F atoms, and (ii) the positional effects by comparing electron and positron TCS for 1,3-difluorobenzene ($1,3$-$C_6H_4F_2$) and 1,4-difluorobenzene ($1,4$-$C_6H_4F_2$) molecules. See Fig. 1 in Ref. [12] for the positions of the two F atoms in these two molecules on the benzene ring. Substitution of all H atoms of the benzene ring by F atoms produces the molecule C_6F_6. We studied both electron and positron TCS [10] and electron impact elastic DCS [11] for these molecules. Substitutional effects following replacement of the benzene H atom(s) by some radical(s) has also been of interest to us for the obvious reason that the nature of the electron donation or extraction between the benzene ring and a radical is expected to be different from that between the benzene ring and an atom. 4-fluorobenzaldehyde ($C_6H_4(CHO)F$), produced by replacement of two H atoms by the radical CHO and an F atom, was the first subject of our study by both electron and positron impact investigating TCS [14]. The most recent work was on H atom substitution by a CH_3 radical to produce toluene ($C_6H_5CH_3$), whereby we investigated electron and positron TCS and electron impact elastic and vibrational excitation DCS [15].

In this paper we report on the experimental measurements of electron and positron TCS and electron impact vibrational excitation DCS for $C_6H_5CF_3$. In particular, we employ the vibrational excitation study as a tool for investigation of the nature and origin of the resonances observed in the TCS. There have been a few works on photoabsorption and infrared and Raman spectra studies on $C_6H_5CF_3$ (see for example [16,17], respectively), but no data that we are aware of for either electron or positron scattering from these molecules.

*Present address: Atomic and Molecular Physics Laboratories, RSPhySE, The Australian National University, Canberra ACT 0200, Australia.

 ©2009 The American Physical Society

II. PROCEDURES

A. TCS experiments

These measurements were carried out using a retarding potential time-of-flight (RP-TOF) method. The apparatus for this has been reported in detail elsewhere [18] and thus only briefly summarized here. The source for the electron and positron beams is a ^{22}Na radioisotope with an activity of ~80 μCi. The energy resolution, solely determined by the RP-TOF experimental apparatus, is an average 0.3 eV below 4 eV, and is impact energy dependent [19]. The TCS values were derived from the Beer-Lambert attenuation equation

$$Q_t = -\frac{1}{n\ell}\ln\frac{I_g}{I_v}, \tag{1}$$

where I_g and I_v refer to the projectile beam intensities transmitted through the collision cell with and without the target gas of number density n, respectively. ℓ refers to the effective length of the collision cell and was established by normalizing our measured positron-N_2 TCS to those of the positron-N_2 data of Hoffman *et al.* [20]. The energy calibration was done using positron-N_2 TOF spectra measured at 20 energies in the energy range 8–150 eV [21]. The $C_6H_5CF_3$ TCS presented in this report were confirmed to be pressure independent in the present energy range by independent electron impact test experiments.

Because of our system's relatively large collision cell entrance- and exit-apertures (i.e., 3 mm in radius) to the geometrical length of 5 cm, there is the possibility of forward scattering problems resulting in our TCS coming out to be smaller than their true values. A detailed method for this correction has been described previously [22,23]. In short, the simulation method for this involves the use of electron/positron DCS for the molecule under study, the cell geometry, magnetic-field strength (4.5 G for electron and 9 G for positron beams) and the position at which the scattering event occurs inside the cell. For these molecules, only electron impact DCS could be found [24] and so the correction could not be carried out for the positron TCS. For electron TCS, the correction resulted in an increase in the TCS magnitude by about 35% at 0.4 eV decreasing with increasing impact energy to about 10% at 10 eV, 5% at 100 eV, and 1% at 1000 eV. It must be noted however that there is large error involved in this correction stemming mainly from the approximation of DCS for the experimentally inaccessible angles $0° \leq \theta \leq 15°$ and $130° \leq \theta \leq 180°$ and the estimation of DCS for TCS energies not covered by the DCS literature, i.e., by assuming the same DCS shape as the nearest energy available from literature DCS, scaled according to the TCS ratio [23]. It is not possible to accurately quantify the error involved in this but we estimate the error in the forward scattering correction amount to be up to 50%.

The errors shown in the data in Table I are the sum total uncertainties made up of contributions from statistical, gas pressure fluctuations and the effective collision cell length calibration. They range 5.5%–6.8% and 6.8%–11.1% for electron and positron impact, respectively. The error due to the forward scattering correction is not included.

B. Vibrational excitation DCS experiments

These experiments were carried out using a crossed beam apparatus, which has already been described previously [25] and thus only briefly summarized here. Incident electrons from a 180° monochromator intercept an effusive molecular beam at right angles and scattered electrons are energy analyzed in a second 180° hemispherical system. In order to maintain reasonably constant electron beam focusing and transmission at the interaction region, programmable power supplies are used to ramp the mid-element potentials of the monochromator exit and analyzer entrance lenses as required. Both the monochromator and the analyzer are enclosed in differentially pumped boxes to reduce the effect of the background gases and to minimize the stray electron background. The target molecular beam is produced by effusing the gas through a nozzle with an internal diameter of 0.3 mm and a length of 5 mm. The spectrometer and the nozzle are heated to a temperature of about 70 °C to reduce the possibility of contamination during measurements. The overall energy resolution of the present measurements was about 40–45 meV and the angular resolution was $\pm 1.5°$.

The vibrational excitation DCS were measured while sweeping the impact energies from 1.5 to 30 eV for the two loss energies 0.160 and 0.384 eV, at a scattering angle of 90°. Absolute cross sections were obtained by the relative flow technique [26] using helium as the reference gas. This involved the measurement of the relative electron scattering intensities for $C_6H_5CF_3$ and helium (He), for which there is an accurate set of DCS. The He cross sections tabulated by Boesten and Tanaka [27] were used. The driving pressures for both the target and reference gases were determined in such a way that their collisional mean free paths are the same in the beam-forming capillary. This is done in order to minimize the effects that collisions have on the relative shapes of the atomic and molecular beams. It is worth noting here, however, that the use of the relative flow requires knowledge of both the target and reference gas collisional diameters [25] in order to establish the correct flow rates. While these were accurately known for He from literature, they had to be estimated for $C_6H_5CF_3$. The estimations were done based on adding the molecular constants for the known CF_4 to C_6H_6 in order to get $C_6H_5CF_3$. The collisional diameter for $C_6H_5CF_3$ so derived was 11.5 Å. The subsequent driving pressures used for the experiments were 0.18 Torr for $C_6H_5CF_3$ and 5 Torr for He. Experimental errors were estimated to be of the order of 15%–20%.

III. RESULTS AND DISCUSSION

Table I shows the numerical values for the electron and positron TCS. A joint electron impact TCS and vibrational excitation DCS study is carried out first. Positron TCS are then discussed, before ending with a comparative study between electron and positron TCS. The C_6H_6 electron and positron TCS presented in Figs. 1 and 5, for the comparative study, have been corrected for the forward scattering effect discussed above.

TABLE I. Benzotrifluoride ($C_6H_5CF_3$) electron and positron TCS($\times 10^{-16}$ cm^2). Electron TCS have been corrected for the forward scattering effect, with the numbers in parentheses showing the values before the correction. Errors are as explained in the text.

Energy (eV)	Electron	Positron	Energy (eV)	Electron	Positron
0.2		35.9 ± 4.0	11	64.0(56.8) ± 3.6(3.2)	37.4 ± 2.7
0.4	75.4(55.7) ± 5.1(3.8)	41.5 ± 4.0	12	62.3(55.1) ± 3.5(3.1)	37.1 ± 2.8
0.6	72.9(57.0) ± 4.5(3.5)	47.8 ± 4.4	13	61.5(53.5) ± 3.0(3.0)	36.7 ± 2.6
0.8	70.6(57.1) ± 4.3(3.5)	46.2 ± 4.0	14	59.5(51.5) ± 2.9(2.9)	35.7 ± 2.7
1.0	67.7(56.4) ± 3.8(3.4)	43.7 ± 3.2	15	58.7(51.7) ± 3.4(3.0)	35.6 ± 2.6
1.2	69.2(56.0) ± 4.1(3.3)		16	56.3(49.6) ± 3.3(2.9)	34.6 ± 2.7
1.3		45.8 ± 3.9	17	56.8(50.0) ± 3.3(2.9)	36.1 ± 2.7
1.4	66.8(54.6) ± 4.0(3.2)		18	56.5(49.7) ± 3.2(2.8)	36.3 ± 2.8
1.6	65.3(53.7) ± 3.9(3.2)	43.4 ± 3.8	19	55.4(48.7) ± 3.2(2.8)	35.5 ± 2.6
1.8	63.2(52.2) ± 3.8(3.2)		20	52.5(47.5) ± 3.2(2.8)	35.3 ± 2.6
1.9		48.4 ± 3.8	22	47.9(45.3) ± 2.7(2.6)	33.9 ± 2.4
2.0	61.6(51.3) ± 3.8(3.2)		25	48.1(45.5) ± 2.7(2.6)	32.6 ± 2.5
2.2	62.4(52.4) ± 3.7(3.1)	45.3 ± 3.7	30	48.5(44.3) ± 2.8(2.5)	33.2 ± 2.3
2.5	60.1(50.7) ± 3.5(3.0)	44.7 ± 3.5	35	46.4(42.5) ± 2.7(2.6)	
2.8	59.0(49.9) ± 3.5(3.0)	44.3 ± 3.6	40	48.9(45.0) ± 2.8(2.6)	33.0 ± 2.3
3.1	57.7(50.3) ± 3.4(3.0)	44.3 ± 3.4	50	47.0(44.1) ± 2.6(2.5)	30.1 ± 2.0
3.4	60.4(52.6) ± 3.6(3.1)	45.0 ± 3.4	60	42.1(39.6) ± 2.3(2.2)	30.8 ± 2.2
3.7	61.2(53.4) ± 3.7(3.2)	45.3 ± 3.2	70	38.6(36.4) ± 2.1(2.0)	29.0 ± 2.2
4.0	62.2(54.2) ± 3.6(3.1)	41.8 ± 2.8	80	38.9(36.6) ± 2.2(2.1)	28.6 ± 2.0
4.5	61.1(53.2) ± 3.4(3.0)	42.8 ± 2.9	90	35.0(33.4) ± 2.0(1.9)	27.5 ± 2.1
5.0	61.9(54.1) ± 3.5(3.1)	41.3 ± 2.9	100	34.4(32.9) ± 1.9(1.9)	27.7 ± 1.9
5.5	63.1(55.8) ± 3.6(3.2)	41.7 ± 2.9	120	31.9(30.6) ± 1.8(1.7)	25.9 ± 1.9
6.0	63.4(56.5) ± 3.7(3.3)	42.4 ± 3.0	150	29.1(28.0) ± 1.6(1.5)	24.4 ± 1.7
6.5	63.4(59.3) ± 3.6(3.4)	40.0 ± 2.8	200	24.5(23.9) ± 1.4(1.3)	24.0 ± 1.8
7.0	62.7(59.2) ± 3.6(3.4)	41.8 ± 3.0	250	22.9(22.4) ± 1.3(1.2)	20.5 ± 1.6
7.5	64.7(61.1) ± 3.7(3.5)	40.2 ± 2.8	300	19.7(19.3) ± 1.1(1.1)	18.5 ± 1.5
8.0	66.1(59.7) ± 3.8(3.5)	37.7 ± 2.8	400	17.7(17.4) ± 1.0(1.0)	16.0 ± 1.4
8.5	66.5(59.9) ± 3.8(3.4)	38.0 ± 2.8	500	15.1(14.8) ± 0.9(0.8)	14.7 ± 1.3
9.0	67.1(60.5) ± 3.9(3.5)	38.5 ± 2.9	600	13.3(13.1) ± 0.8(0.7)	12.5 ± 1.2
9.5	64.3(58.2) ± 3.8(3.4)	40.3 ± 3.0	800	9.7(9.6) ± 0.5(0.5)	11.0 ± 0.8
10	63.1(57.1) ± 3.6(3.3)	39.1 ± 2.8	1000	8.5(8.4) ± 0.5(0.5)	8.8 ± 0.7

A. Electron impact

1. TCS

Figure 1(a) shows the current electron impact TCS results measured over the energy range 0.4–1000 eV, in comparison with those of C_6H_6 [10] from our previous publication. The qualitative similarities between the current TCS with those for C_6H_6 include the minimum centered at ~3 eV, the main peak at 8.0 eV, the shoulder at about 40 eV, and the monotonous decrease toward 1000 eV, i.e., from about 62 $\times 10^{-16}$ cm^2 at 8 eV down to about 8×10^{-16} cm^2 at 1000 eV. Substitution of an H atom in C_6H_6 by the CF_3 radical destroys the symmetry of the benzene ring, i.e., making the resulting molecule $C_6H_5CF_3$ dipolar (2.86 D). This dipole moment is expected to induce long-range scattering causing TCS to rise with decreasing electron energy toward 0 eV, as

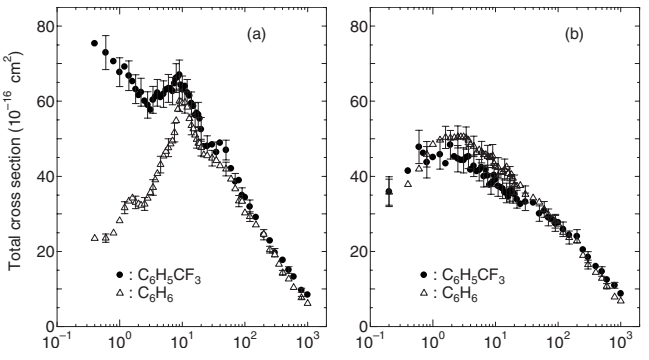

FIG. 1. Electron (a) and positron (b) TCS for $C_6H_5CF_3$ compared with those for C_6H_6 from our previous publication [10].

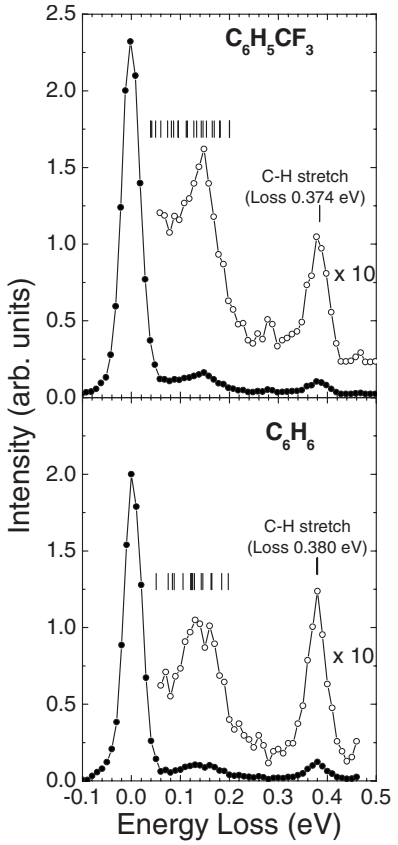

FIG. 2. $C_6H_5CF_3$ electron impact energy-loss spectrum at impact energy 7.5 eV and scattering angle 90° compared with a similar spectrum for C_6H_6. The vertical bars indicate positions of 24 of the 30 known fundamental vibrational mode frequencies (energies) [17]. See Table II.

observed below 3 eV. The decreasing TCS magnitude trend above 10 eV is due to the decreasing time the electron has for interaction with the molecule as its velocity increases. Compared to C_6H_6 TCS, $C_6H_5CF_3$ TCS are up to 3 orders of magnitude greater below 10 eV, pointing to the role of the long-range interaction in the latter compared to the former. Above 10 eV, $C_6H_5CF_3$ TCS are marginally greater than those for C_6H_6. Although both molecules show a shoulder at about 40 eV, this is more pronounced for $C_6H_5CF_3$. It remains unclear what the origin of this feature is. In order to investigate the origin and nature of the 8.0 peak we carried out vibrational excitation experiments, i.e., the inelastic channel often associated with resonance features of this nature.

2. Probing the resonances in the TCS: vibrational excitation DCS

Figure 2 shows the electron-energy-loss spectrum for the impact energy of 7.5 eV and scattering angle of 90° compared with a similar spectrum for C_6H_6. $C_6H_5CF_3$ molecules have 30 fundamental and 4 CF_3 vibrational modes, 24 of which are indicated by the dashed vertical bars in Fig. 2 and shown in Table II. See Ref. [17] for the complete list and individual characteristics of each mode.

The results we show in Fig. 3 are for the vibrational excitation at the energy losses of 0.160 and 0.384 eV, chosen because they represent the dominant modes. It is worth pointing out though that, because of our energy resolution of about 40 meV, the loss energy setting of 0.160 eV for our apparatus inevitably includes the seven modes falling within the 0.160 ± 20 meV energy window, i.e., the two C-H bending (a_1 symmetry at loss energy 0.146 eV, b_1 symmetry at 0.153 eV), the three ring deformation (b_1 symmetry at loss energy 0.169 eV, a_1 and b_1 symmetries at 0.181 eV), the asymmetric CF_3 deformation (at loss energy 0.143 eV), and the symmetric CF_3 deformation (at loss energy 0.165 eV) modes. Hence the following discussions of the 0.160 eV loss energy spectra ought to be taken to mean a mixture of these seven vibrational modes. Similarly, the setting of our apparatus for measurements at the energy loss of 0.384 eV inevitably means both the a_1 and b_1 symmetries of the C-H stretching mode are included, i.e., since they are both observed at the same loss energy of 0.384 eV, and thus the

TABLE II. Configurations of the vibrational modes of $C_6H_5CF_3$ molecules from Ref. [17].

Vibrational mode	Energy (eV)	Species	Vibrational mode	Energy (eV)	Species
Ring deformation	0.042	a_1	Ring deformation	0.200	b_1
Ring breathing	0.095	a_1	C-H stretch	0.384	b_1
C-CF_3 stretching	0.127	a_1	Ring deformation	0.060	b_2
C-H bending	0.133	a_1	Ring deformation	0.086	b_2
C-H bending	0.146	a_1	C-H bending	0.095	b_2
Ring deformation	0.181	a_1	C-H bending	0.114	a_2
Ring deformation	0.200	a_1	CF_3 rocking	0.039	
C-H stretching	0.384	a_1	CF_3 rocking	0.049	
C-H bending	0.112	b_1	Asymmetric-CF_3 deformation	0.074	
C-H bending	0.153	b_1	Symmetric-CF_3 deformation	0.081	
Ring deformation	0.169	b_1	Asymmetric-CF_3 stretching	0.143	
Ring deformation	0.181	b_1	Symmetric-CF_3 stretching	0.165	

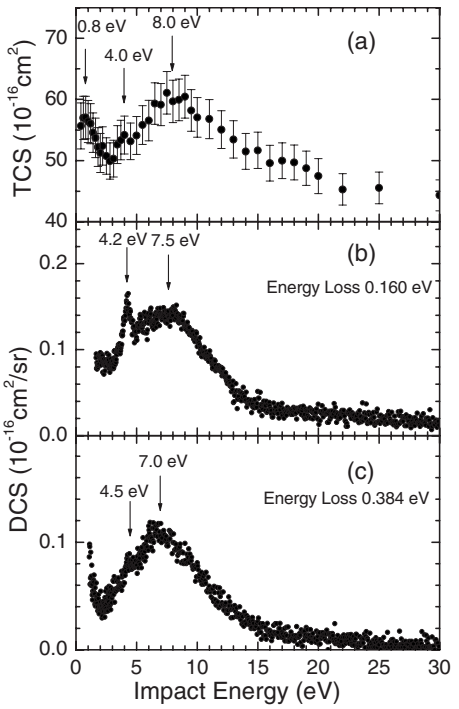

FIG. 3. $C_6H_5CF_3$ electron impact (a) TCS and vibrational excitation DCS functions for the two loss energies (b) 0.160 eV and (c) 0.384 eV at impact energies of 1.5–30 eV and scattering angle 90°.

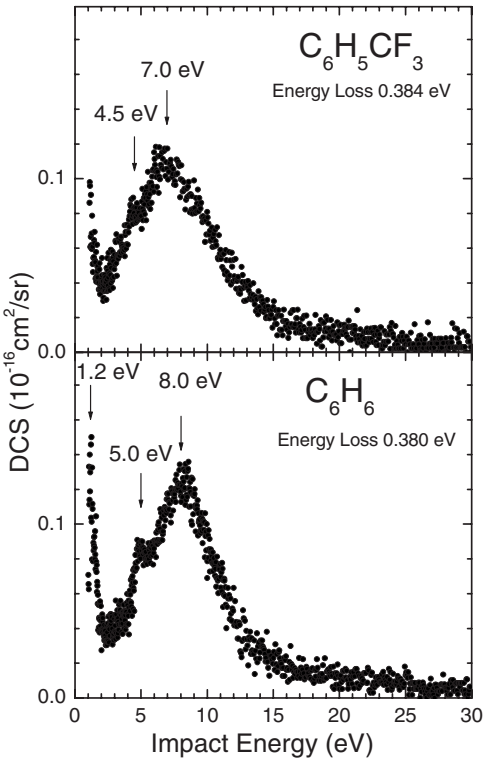

FIG. 4. $C_6H_5CF_3$ electron impact vibrational excitation DCS functions for the loss energy 0.384 eV at impact energies of 1–30 eV and scattering angle 90° compared with similar results for C_6H_6.

following discussions of the 0.384 eV spectra should be taken to mean a combination of the two.

The results in Fig. 3 show clear energy dependence agreement between the two vibrational excitation spectra and the TCS. We summarize the observations as follows. (i) The 0.160 eV loss energy vibrational excitation DCS show a peak centered at about 4.2 eV and a rather broad one at 7.5 eV, i.e., in agreement with the TCS peak which is centered 8 eV. (ii) The 0.384 eV loss energy vibrational excitation DCS spectra are characterized by the rising trend at 1.5 eV, albeit not yet a peak, a shoulder at about 4.5 eV and the main peak at 7 eV, again in agreement with the TCS peak position at 8 eV. The TCS peak spanning the energy region from 5 to 15 eV seems to be a resonance feature composed of contributions from a mixture of all these vibrational excitations, i.e., seven observed at loss energy 0.160 eV and two at 0.384 eV. In addition, it is important to note that Allan [28], in an extensive experimental study of C_6H_6, observed three resonance peaks centered at 1.13, 4.8, and 8.5 eV. He reported them to be due to the $^2E_{2u}$, $^2B_{2g}$, and $^2E_{1u}$ shape resonances resulting from the temporary capture of an incident electron into the $\pi^*(e_{2u})$, $\pi^*(b_{2g})$, and $\sigma^*(e_{1u})$ orbitals, respectively. We thus infer the same and attribute the peak we observe at 8.0 eV to the $^2E_{1u}$ shape resonance. This deduction on the assignment of the symmetries to this resonance is also supported by the similarity in the vibrational excitation of the same symmetric and asymmetric C-H stretching mode spectra observed between the current results for $C_6H_5CF_3$ and those for C_6H_6 as shown in Fig. 4. We think that the shoulder observed at about 40 eV in the TCS should have stronger contributions from other scattering channels than the vibrational excitation, most likely ionization. It must be noted though that the vibrational excitation cross sections presented here are only differential functions, i.e., not integral, and that they are about 2 orders of magnitude smaller so that their actual contributions to the TCS may not be obvious.

In Fig. 4 we show the vibrational excitation DCS functions for the ring symmetric and asymmetric C-H stretching modes of $C_6H_5CF_3$ together with those for C_6H_6, i.e., all studied over the same energy range 1–30 eV and scattering angle of 90°. The resonance peaks observed at about 1, 4.5, and 7.0 eV in $C_6H_5CF_3$ are observed at 1.2, 5.0, and 8.0 eV in C_6H_6, and at 1.4, 5.0, and 7.5 eV in $C_6H_5CH_3$ [15] (not shown). We consider this to mean that the attachment of the CF_3, or CH_3, radical to the benzene ring hardly affects the resonances due to the symmetric and asymmetric C-H stretching vibrational modes.

B. Positron TCS

In Fig. 1(b) we show the $C_6H_5CF_3$ positron TCS in comparison with those of the parent C_6H_6 molecule. The qualitative similarity between these two sets of TCS is obvious. These include (i) the gradual decrease below 1 eV, i.e., in contrast to the slowly rising trend in the electron TCS counterpart at this energy range, (ii) observation of broad peaks commonly centered at about 2 eV, (iii) unclear features in the region 0.6–20 eV, and (iv) the shoulder centered at about 50 eV. However, it is important to note here that because these $C_6H_5CF_3$ TCS have not been corrected for the forward scattering effect, the trend observed below 10 eV may not be definitive. This is because, from our experience with the ex-

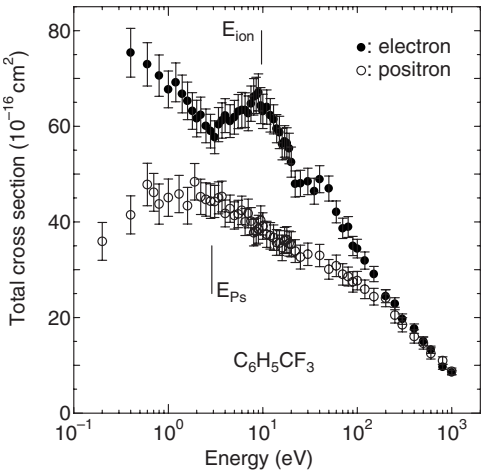

FIG. 5. Electron and positron TCS for $C_6H_5CF_3$ molecules. The vertical lines labeled E_{ion} and E_{Ps} indicate the threshold energy positions for ionization and positronium formation, respectively.

tent to which TCS can be affected by this effect, positron TCS can be affected more due to the use of stronger magnetic field (twice that for electron impact). That is, though the results presented in Fig. 1(b) do not show a turn for the rise, as expected because of the permanent dipole moment (2.86 D) giving rise to a long-range interaction at these low energies, it is possible that after the forward scattering correction a rising trend could be observed. The $C_6H_5CF_3$ TCS are lower than those of C_6H_6 between about 1 and 100 eV. This is intriguing because $C_6H_5CF_3$ is larger in terms of the molecular size, and thus it would be expected to have a larger number of rovibrational states which should make it have larger TCS at these lower energies. This intuition however is true for the electron TCS case. Above 100 eV, however, $C_6H_5CF_3$ TCS gradually become greater than those of C_6H_6, albeit still within experimental errors. Whereas it was possible to present detailed discussions of the electron TCS features because of the availability of the experimental vibrational excitation DCS, it is not possible to do the same here because of the unavailability of any partial cross sections for positron impact from these molecules.

C. Comparative study of positron with electron TCS

Figure 5 shows the present $C_6H_5CF_3$ positron and electron TCS. As already highlighted above, electron TCS rise rapidly below 3 eV compared to a decreasing one for positron impact, i.e., despite the fact that both are expected to show a rising trend due to the dipole induced long-range interaction.

The threshold for positronium formation, E_{Ps}, for $C_6H_5CF_3$ is 2.89 eV [29], and thus positronium formation cannot be contributing to the initial rise in the TCS to produce this peak centered at 0.8 eV for positron impact. Thus, it is reasonable to assume that this phenomenon is related to rovibrational excitation of these molecules. The opening up of the ionization channel at E_{ion} (9.685 eV) is not followed by any clear rising of the TCS for both electron and positron impact. TCS for both projectiles seem to show the change of slope at 40–50 eV, more pronounced for electron impact, before the common monotonous decrease until, within experimental errors, they nearly equal each other above 200 eV. This merging of the TCS is expected since at these higher energies only the long-range interaction dominates the scattering event with the result that only the first Born term is sufficient for describing the scattering, where the square of the charge of the incoming particle comes into the cross-section formula leading to this convergence phenomenon in electron and positron TCS. The absence of resonances in positron scattering is clearly observed in the low to intermediate energy ranges where the TCS for electron impact are always larger by nearly more than a factor at all energies below 200 eV.

IV. CONCLUSION

In this paper $C_6H_5CF_3$ electron and positron scattering cross sections are reported. Electron TCS showed a rising trend below 3 eV, expected for these polar molecules due to the long-range interaction, compared to a decreasing trend for positron. A peak and shoulder were observed in the electron TCS 8.0 and 40 eV, respectively. The origin of the 8 eV peak was probed by means of vibrational excitation experiments and found to have some origin in this channel, attributed to the $^2E_{1u}$ shape resonance, inferred from the literature results of the parent C_6H_6 molecule. Positron TCS showed broad peaking in the energy range 0.8–15 eV, and a shoulder at 40–50 eV, before gradually decreasing toward 1000 eV. The effect of the CF_3 substitution for the benzene H atom showed up as (i) larger $C_6H_5CF_3$ TCS over the whole energy range for electron TCS, and as (ii) lower $C_6H_5CF_3$ TCS than C_6H_6 at 1–100 eV for positron impact. The tendency toward merging of the electron and positron $C_6H_5CF_3$ TCS above 200 eV is rather expected from the first Born approximation.

ACKNOWLEDGMENTS

This work was supported in part by a Grant-in-Aid from the Ministry of Education, Science, Technology, Sport and Culture, Japan, the Japan Society for the Promotion of Science (JSPS), and a Cooperative Research Grant from the National Institute for Fusion Science (NIFS).

[1] M. Matsuzawa, J. Phys. Soc. Jpn. **18**, 1473 (1963).
[2] F. H. Read and G. L. Whiterod, Proc. Phys. Soc. **85**, 71 (1965).
[3] W. E. Wentworth, L. W. Kao, and R. S. Becker, J. Phys. Chem. **79**, 1161 (1975).
[4] L. G. Christophorou, R. P. Blaunstein, and D. Pittman, Chem. Phys. Lett. **22**, 41 (1973).
[5] H. Shimamori, Y. Tatsumi, and T. Sunagawa, J. Chem. Phys. **99**, 7787 (1993).
[6] J.-F. Gal, S. Geribaldi, G. Pfister-Guillouzo, and D. G. Morris, J. Chem. Soc., Perkin Trans. 2 **1985**, 103.
[7] L. G. Christophorou, D. L. McCorkle, and J. G. Carter, J. Chem. Phys. **60**, 3779 (1974).
[8] S. L. Lunt, D. Field, S. V. Hoffmann, R. J. Gulley, and J.-P. Ziesel, J. Phys. B **32**, 2707 (1999).
[9] J. K. Olthoff, J. A. Tossell, and J. H. Moore, J. Chem. Phys. **83**, 5627 (1985).
[10] C. Makochekanwa, O. Sueoka, and M. Kimura, Phys. Rev. A **68**, 032707 (2003).
[11] H. Cho, R. J. Gulley, K. Sunohara, M. Kitajima, L. J. Uhlmann, H. Tanaka, and S. J. Buckman, J. Phys. B **34**, 1019 (2001).
[12] C. Makochekanwa, O. Sueoka, and M. Kimura, J. Phys. B **37**, 1841 (2004).
[13] C. Makochekanwa, O. Sueoka, and M. Kimura, J. Chem. Phys. **119**, 12257 (2003).
[14] O. Sueoka, C. Makochekanwa, and H. Kawate, Nucl. Instrum. Methods Phys. Res. B **192**, 206 (2002).
[15] H. Kato, C. Makochekanwa, Y. Shiroyama, M. Hoshino, N. Shinohara, O. Sueoka, M. Kimura, and H. Tanaka, Phys. Rev. A **75**, 062705 (2007).
[16] *Higher Excited States of Polyatomic Molecules*, edited by M. R. Robin (Academic, New York, 1975), Vol. 2.
[17] N. A. Narasimham, J. R. Nielsen, and R. Theimer, J. Chem. Phys. **27**, 740 (1957).
[18] O. Sueoka, S. Mori, and A. Hamada, J. Phys. B **27**, 1453 (1994).
[19] M. Kimura, C. Makochekanwa, and O. Sueoka, J. Phys. B **37**, 1461 (2004).
[20] K. R. Hoffman, M. S. Dababneh, Y. F. Hsieh, W. E. Kauppila, V. Pol, J. H. Smart, and T. S. Stein, Phys. Rev. A **25**, 1393 (1982).
[21] O. Sueoka and S. Mori, J. Phys. B **19**, 4035 (1986).
[22] A. Hamada and O. Sueoka, J. Phys. B **27**, 5055 (1994).
[23] O. Sueoka, C. Makochekanwa, H. Tanino, and M. Kimura, Phys. Rev. A **72**, 042705 (2005).
[24] H. Kato, M. C. Garcia, T. Asahina, M. Hoshino, C. Makochekanwa, H. Tanaka, F. Blanco, and G. Garcia, Phys. Rev. A **79**, 062703 (2009).
[25] H. Tanaka, T. Ishikawa, T. Masai, T. Sagara, L. Boesten, M. Takekawa, Y. Itikawa, and M. Kimura, Phys. Rev. A **57**, 1798 (1998).
[26] S. K. Srivastava, A. Chutjian, and S. Trajmar, J. Chem. Phys. **63**, 2659 (1975).
[27] L. Boesten and H. Tanaka, At. Data Nucl. Data Tables **52**, 25 (1992).
[28] M. Allan, J. Electron Spectrosc. Relat. Phenom. **48**, 219 (1989).
[29] *CRC Handbook of Chemistry and Physics*, edited by David R. Lide, 81st ed. (CRC, New York, 2000).